

1
2
3
4
5
6
7
8
9
10
11
12
13
14
15
16
17
18
19
20
21
22
23
24
25
26
27

Article type : Review

Systematic review and patient-level meta-analysis of SARS-CoV-2 viral dynamics to model response to antiviral therapies

Silke Gastine ¹, Juanita Pang ², Florencia A.T. Boshier ², Simon J. Carter ¹, Dagan O. Lonsdale ^{3,4}, Mario Cortina-Borja ⁵,
Ivan F.N. Hung ⁶, Judy Breuer ², Frank Kloprogge ⁷, Joseph F. Standing ¹

¹ Infection, Immunity and Inflammation Research and Teaching Department, Great Ormond Street Institute of Child Health, University College London, London, United Kingdom

² Division of Infection and Immunity, University College London, London, United Kingdom

³ Department of Clinical Pharmacology, St George's University of London, United Kingdom

⁴ Department of Intensive Care, St George's University Hospitals NHS Foundation Trust, London, United Kingdom

⁵ Population, Policy and Practice Research and Teaching Department, Great Ormond Street Institute of Child Health, University College London, London, United Kingdom

⁶ Division of Infectious Diseases, Department of Medicine, The University of Hong Kong, Hong Kong, China

⁷ Institute for Global Health, University College London, London, United Kingdom

Running title: Covid Antiviral Modelling

Key words: SARS-CoV-2, COVID-19, viral dynamics, pharmacodynamics

This article has been accepted for publication and undergone full peer review but has not been through the copyediting, typesetting, pagination and proofreading process, which may lead to differences between this version and the [Version of Record](#). Please cite this article as [doi: 10.1002/CPT.2223](#)

This article is protected by copyright. All rights reserved

28 SOURCE OF FUNDING

29 No specific funding was available for this work. Support at institution level came from the National Institute for Health
30 Research Biomedical Research Centre at Great Ormond Street Hospital for Children NHS Foundation Trust and
31 University College London, and J.F.S. and F.K. were supported by United Kingdom Medical Research Council (MRC)
32 Fellowships (grants M008665 and P014534). JB receives funding from the NIHR UCL/UCLH Biomedical Research
33 Centre. JP is supported by a Rosetrees Trust PhD fellowship (M876). FTB is supported by a Wellcome Trust
34 Collaborative Award (203268) to JB.

35

36 DISCLOSURE OF CONFLICT OF INTEREST

37 The authors declared no competing interests for this work. As an Associate Editor of Clinical Pharmacology and
38 Therapeutics, Joseph F. Standing was not involved in the review or decision process for this paper.

39

40

41 Corresponding Author:

42 Dr Silke Gastine

43 Infection, Immunity & Inflammation, Great Ormond Street Institute of Child Health, University College London, London,
44 WC1N 1EH, United Kingdom

45 Email: s.gastine@ucl.ac.uk

46

47

48

49

50

51 ABSTRACT

52 SARS-CoV-2 viral loads change rapidly following symptom onset so to assess antivirals it is important to understand the
53 natural history and patient factors influencing this. We undertook an individual patient-level meta-analysis of SARS-CoV-
54 2 viral dynamics in humans to describe viral dynamics and estimate the effects of antivirals used to-date. This systematic
55 review identified case reports, case series and clinical trial data from publications between 1/1/2020 and 31/5/2020
56 following PRISMA guidelines. A multivariable Cox proportional hazards regression model (Cox-PH) of time to viral
57 clearance was fitted to respiratory and stool samples. A simplified four parameter nonlinear mixed-effects (NLME) model
58 was fitted to viral load trajectories in all sampling sites and covariate modelling of respiratory viral dynamics was
59 performed to quantify time dependent drug effects. Patient-level data from 645 individuals (age 1 month-100 years) with
60 6316 viral loads were extracted. Model-based simulations of viral load trajectories in samples from the upper and lower
61 respiratory tract, stool, blood, urine, ocular secretions and breast milk were generated. Cox-PH modelling showed longer
62 time to viral clearance in older patients, males and those with more severe disease. Remdesivir was associated with faster
63 viral clearance (adjusted hazard ratio (AHR) = 9.19, $p < 0.001$), as well as interferon, particularly when combined with
64 ribavirin (AHR = 2.2, $p = 0.015$; AHR = 6.04, $p = 0.006$). Combination therapy should be further investigated. A viral
65 dynamic dataset and NLME model for designing and analysing antiviral trials has been established.

66 INTRODUCTION

67 Finding antivirals that target severe acute respiratory syndrome coronavirus 2 (SARS-CoV-2) will be crucial in managing
68 the ongoing pandemic. In addition to the development of novel agents, substantial efforts are underway to establish
69 whether currently available agents may be re-purposed¹. A key biomarker for clinical antiviral activity is viral load in
70 bodily fluids and assessing a drug's or drug combination's ability to reduce viral load is an important first step in
71 identifying therapies that influence clinical outcome.

72
73 To correctly assess antiviral activity, it is first necessary to understand viral load natural history. As a rapidly progressing,
74 primarily respiratory viral infection, SARS-CoV-2 elimination from the body seems to be mainly driven by a combination
75 of innate immune response and exhaustion of target cells available for infection². Observational cohort studies published
76 to date have shown that the rate of viral load decline seems slower in older patients, those with more severe disease and
77 those with comorbidities such as diabetes mellitus and immunosuppression^{3, 4, 5, 6}. Interpreting these observational studies
78 requires caution because patients have often received antiviral therapies. Due to the time point of initial infection being
79 unknown, assessing viral load in response to treatment must account for time since symptom onset⁷.

80
81 Since February 2020 case reports and case series of patient-level viral dynamics have been published, some of which
82 report dosing of antiviral drugs⁸. Clinical trials of antivirals and their association with viral load are also beginning to read
83 out⁹. Meanwhile large pragmatic trials of repurposed monotherapy antivirals have yet to find a clearly effective agent¹⁰. At
84 this crucial juncture, it is vital to develop a pharmacodynamic modelling framework that can be used to describe the
85 natural history of SARS-CoV-2 viral dynamics, make initial estimates on antiviral efficacy of agents used to-date, and to
86 design and evaluate Phase II trials using viral load as a biomarker.

87
88 This systematic review therefore aimed to search for case reports, case series and clinical trials reporting serial individual
89 patient-level SARS-CoV-2 viral load measurements in humans from any sampling site upon which an individual patient-
90 level meta-analysis was then performed. A nonlinear mixed effects (NLME) viral dynamic model was fitted to describe
91 the viral trajectories in each sampling site and to give a quantitative measure of viral dynamics. In data of sufficient
92 quality, the parameters of multivariable Cox proportional hazards regression models of time to viral clearance, and NLME
93 models of antiviral efficacy were estimated.

94 METHODS

95 **Protocol and registration**

96 The protocol for this systematic review and individual patient meta-analysis, which follows the PRISMA Individual
97 Patient Data systematic reviews guideline¹¹, was first published on 27/5/2020 at: [https://github.com/ucl-](https://github.com/ucl-pharmacometrics/SARS-CoV-2-viral-dynamic-meta-analysis)
98 [pharmacometrics/SARS-CoV-2-viral-dynamic-meta-analysis](https://github.com/ucl-pharmacometrics/SARS-CoV-2-viral-dynamic-meta-analysis). The final dataset and statistical analysis code are also
99 published here. The review was registered with PROSPERO (CRD42020189000).

100

101 **Eligibility criteria**

102 This study aimed to identify serial viral loads with time in human subjects infected with SARS-CoV-2 in order to describe
103 and model viral load trajectory. The inclusion criteria were therefore papers containing individual subject-level reports of
104 viral load with time, either since symptom onset or time since start of monitoring for asymptomatic subjects, and sampling
105 site. Authors of manuscripts describing summary statistics of viral load with time were contacted requesting participant
106 level data. Viral load was defined as either a value in copies/mL or a cycle threshold (Ct) value of an uncalibrated
107 polymerase chain reaction (PCR) assay.

108

109 **Overall search strategy**

110 Since SARS-CoV-2 was notified to the WHO on 31/12/2019, we did not expect to find relevant papers published prior to
111 this date. Hence, PubMed, EMBASE, medRxiv, and bioRxiv were searched with a date range of 1/1/2020 to 31/5/2020.
112 The following search terms were used for PubMed and EMBASE: (SARS-CoV-2 OR COVID OR coronavirus OR 2019-
113 nCoV) AND (viral load OR cycle threshold OR rtPCR OR real-time PCR OR viral kinetics OR viral dynamics OR
114 shedding OR detection OR clinical trial). Due to character limits in the search engine, the following search terms were
115 used for medRxiv and bioRxiv: (SARS-CoV-2 OR COVID-19 OR coronavirus) AND (viral load OR cycle threshold OR
116 PCR OR viral dynamics OR clinical trial).

117

118 After removing duplicates, two reviewers independently identified papers for full text screening, with any discrepancies
119 resolved by a third reviewer.

120

121 **Data extraction**

122 Viral loads were reported as either numerical values in tables, figures, or in viral load *versus* time plots. Where possible,
123 numerical values were copy-pasted directly into a comma separated value (csv) format from the source, whereas tabulated

124 numerical values contained in pdf images were extracted using <https://extracttable.com/>. Viral loads reported in plots were
125 extracted using Web Plot Digitizer¹².

126

127 Each viral load was paired with a time since symptom onset or in asymptomatic subjects, the time since viral monitoring
128 started. Furthermore, sampling site and, if viral load not reported in copies/mL, the PCR assay including the primers used,
129 were extracted along with limit of quantification and limit of detection, if available. The following patient-level covariates
130 were extracted if available:

- 131 • Presence of fever >37.5 °C at any time (non-time varying covariate)
- 132 • age, where possible individual age but otherwise the study's reported central measure (e.g. mean, median)
- 133 • sex or the male/female ratio was extracted if patient-level data not reported
- 134 • need for and days of intensive care treatment
- 135 • need for and days of mechanical ventilation
- 136 • whether patient died and time to death from symptom onset.

137 In addition, a standardised disease score was constructed for each patient as follows:

138 0 - asymptomatic

139 1 - mild disease (fever, cough or other mild symptoms reported)

140 2 - moderate disease (in addition to mild criterion: need for supplemental oxygen /non-invasive ventilation)

141 3 - severe disease (requirement for mechanical ventilation)

142 All data were stored on a shared github repository, and standardised R-scripts took data from each paper to merge into a
143 single master dataset. A quality control (QC) check on viral load values and all covariates was performed for each paper
144 by an independent reviewer.

145

146 **Data quality assessment**

147 Viral load quality score

148 Two quality assessments were applied to each dataset. Firstly, the quality of viral load reporting was rated on a 1-3 scale.
149 The highest quality 1 was assigned to studies reporting viral load in copies/mL or reporting a calibration curve allowing
150 for direct conversion of Ct values to viral load. Quality 2 was assigned if viral load was reported in PCR Ct and primers
151 used in the assay were reported, but calibration data was missing. In this case a published calibration curve for that primer
152 from another source was used to convert to viral load in copies/mL^{13, 14}. Where more than one calibration curve was
153 available for the same primer the mean slope and intercept was used. The lowest (quality score 3) was assigned when viral

154 load was reported in PCR Ct but no further information was available on the PCR assay. In this instance a conversion to
155 copies/mL was made using the mean slope and intercepts from all calibration curves.

156

157 Drug quality score

158 The second quality assessment on a 3-point scale related to reporting of the antiviral drug therapy administered: which
159 drug(s) and upon which days did patients receive the drug(s). The highest quality 1 was assigned when it was reported
160 which days each patient received each drug, or these data were provided by corresponding authors. If it was reported that
161 no antiviral was administered this was also assigned quality 1. Quality 2 was assigned when antiviral drug treatment was
162 reported, but ascertaining which days the patient had received the drugs was not possible. The lowest category, quality 3,
163 was assigned when it was not possible to determine whether or not antivirals had been administered.

164

165 **Statistical analysis**

166 Primary analysis of time to viral clearance using Cox proportional hazards modelling

167 The primary analysis was conducted on observed time to viral clearance, which was analysed fitting Cox proportional
168 hazards regression models with adjusted hazard ratios estimated for each covariate. We verified the assumptions of
169 proportional hazards using the Therneau-Grambsch test.¹⁵ The data used for this analysis were limited to respiratory and
170 stool sampling sites only, as virus was found to be mostly undetectable at other sites. Furthermore, only data from patients
171 with known antiviral history (drug quality 1 and 2) were used. To assess the possible risk of bias in different drug and viral
172 load qualities, the analysis was repeated on two further subsets: Firstly, with only drug quality 1 and respiratory samples,
173 and secondly on assay quality 1 data only.

174

175 Time to viral load dropping below the limit of detection was modelled with Cox proportional hazards regression in R
176 (version 3.6.3)¹⁶. Where a single patient contributed samples from multiple sampling sites (e.g. upper respiratory and
177 stool), the time to the last site testing negative was used. Multivariable models for covariate effects on time to viral
178 clearance were fitted, with additional interaction terms for drug therapies included, where multiple antiviral agents were
179 given simultaneously. In studies reporting sex as a proportion of males, 10 000 datasets were simulated using the reported
180 fraction of males to randomly assign individuals to being male from the binomial distribution. The Cox proportional
181 hazards regression model was then fitted to each dataset and parameter estimates compared with the model, where
182 individual sex was assigned by rounding the fraction of males. Model parameter estimates were visualised using forest
183 plots.

184 Secondary analysis antiviral pharmacology model

185 The secondary analysis was to use a NLME model to quantify the increase in viral elimination rate with antiviral therapy.

186 This analysis used data only from respiratory samples and rated drug quality 1.

187 *Nonlinear mixed-effects (NLME) viral dynamic model*

188 Firstly, a descriptive analysis of all data was undertaken. A NLME viral dynamics model was fitted to the individual
189 patient-level viral load *versus* time data. The structural model was based on the general target cell limited model, which
190 has previously been used to describe respiratory viral infections^{7, 17}. This model consists of three ordinary differential
191 equations relating to changes in uninfected target cells (T), infected target cells (I) and free virus (V) over time (t), as
192 follows:

193
$$\frac{dT(t)}{dt} = -\beta T(t)V(t)$$

194
$$\frac{dI(t)}{dt} = \beta T(t)V(t) - \delta I(t)$$

195
$$\frac{dV(t)}{dt} = \rho I(t) - cV(t)$$

196 where β is the rate at which target cells become infected in the presence of virus, δ is the death rate of infected cells, ρ is
197 the rate of viral production from infected cells and c is the rate of clearance of free virus. This model is structurally
198 unidentifiable, as tested through the *IdentifiabilityAnalysis* package in Wolfram Mathematica 12.1 (Wolfram Research,
199 Illinois, USA)¹⁸, unless the initial condition for T , β , or ρ are known. Furthermore, the elimination rate of free virus (c) is
200 likely to be much faster than the death rate of infected cells (δ). Hence, by assuming a quasi-steady-state between I and V ,
201 and normalising the total cell number by the number of infected cells when observations begin ($t = 0$), it is then possible to
202 reduce the model to a structurally identifiable, two state ordinary differential equation model relating to the fraction (f) of
203 infected cells with time and infected cells as a proxy for viral load as follows¹⁹:

204
$$\frac{df(t)}{dt} = -\beta f(t)V(t)$$

205
$$\frac{dV(t)}{dt} = \gamma f(t)V(t) - \delta V(t)$$

206 with γ , a new parameter equal to $\rho\beta T_0/c$ and interpreted to be the maximum rate of viral replication. δ can now be
207 interpreted as overall viral elimination rate. This population model was then fitted to viral load data with time using the
208 following form:

209
$$y_{ij} = f(\varphi_i, t_{ij}) + \varepsilon_{ij}$$

210 where y_{ij} was the viral load from subject i at time t_{ij} , f is the nonlinear model defined above with parameters ϕ_i , and ε_{ij} the
211 residual between the model prediction and the observed data.

212

213 Four parameters were estimated: the initial viral load at symptom onset (V_0), β , δ and γ . Interindividual variability was
214 estimated for V_0 , β and δ with each assumed to follow a log-normal distribution. Viral loads were log transformed and the
215 residual error was assumed to follow a normal distribution. Parameter estimation by maximum likelihood was undertaken
216 using the stochastic approximation expectation maximization (SAEM) in NONMEM version 7.4²⁰. Model evaluation was
217 undertaken by analysis of normalised prediction distribution errors (NPDE) and visual predictive checks (VPC)²¹. Viral
218 loads below the limit of detection (LOD) were included by integrating the density function from minus infinity to the limit
219 of detection to yield a probability of the data being below the LOD (“M3 Method”)²².

220 In some participants, multiple samples were taken at the same time point (either different sampling site or the same sample
221 assayed by more than one method). In this case a common residual error term was used to allow for modelling one-level
222 nested random effects.

223

224 *Descriptive analysis of viral shedding by sample site*

225 The above model was fitted to data from each sampling site. The resulting parameters were then used to simulate the
226 overall population viral load trajectories. For the respiratory sample sites viral area under the curve (AUC), peak viral load
227 and half-life were derived from the model and plotted *versus* patient covariates.

228 *Covariate analysis and antiviral drug effects modelling*

229 The initial model used only data obtained in untreated patients. A covariate analysis was undertaken testing the influence
230 of sampling site (nasal *versus* oral *versus* lower respiratory tract), sex, age and disease status on either V_0 , β or δ .
231 Covariates were retained in the model based on the likelihood ratio test with a threshold level of significance of $p < 0.01$,
232 and if the same covariate addition to V_0 , β or δ all gave significant improvement to model fit then the model with the
233 largest decrease in $-2 \log$ likelihood (NONMEM objective function value (OFV)) was chosen. For the final model viral
234 area under the curve (AUC), peak viral load and half-life were derived and plotted *versus* patient covariates.

235

236 Using the final demographic model, data from patients undergoing antiviral treatment (antiviral drug quality 1) were
237 added. A univariable analysis was performed, testing each drug’s ability to increase δ . Drugs showing significant
238 improvement in model fit ($p < 0.01$), according to the likelihood ratio test, were then included in the final multivariable
239 model.

241 Simulations based on the antiviral pharmacology model

242 Simulations were performed to explore the change in viral trajectories for different time points of therapy initiation: Day 1
243 after symptom onset, Day 3, Day 7 and Day 10. Interferon and ribavirin monotherapy along with the combination therapy
244 interferon plus ribavirin were explored this way. A dummy population of 5100 subjects with ages uniformly distributed
245 across 50 to 100 years, consisting of an equal ratio of males and females was created. Each regimen was simulated using
246 the entire population, assuming sampling from the upper respiratory tract or nose for a time window of 14 days.
247 Comparisons of the sample size required to detect a significant difference in the proportion of undetectable virus between
248 antiviral and no treatment were made after 7 days of treatment with a 90% power and alpha level of $p < 0.05$ for antivirals
249 starting at Days 1, 3 and 7 post symptom onset.

250 RESULTS

251 Results of the systematic search are given in Figure 1, and details of included papers in Table 1. Individual patient-level
252 data were extracted from 45 articles reporting viral loads and/or PCR Ct values with time since symptom onset. Of these
253 32 papers either reported antiviral participant-level drug histories, or these were provided by the corresponding author.
254 The full dataset contained 645 individuals contributing 6316 viral load samples. The majority of samples (n) were taken
255 from the respiratory tract: nasopharyngeal (315 individuals, $n=2208$), oropharyngeal or saliva (381 individuals, $n=2144$)
256 and lower respiratory tract (81 individuals, $n=799$). The other reported samples sites were stool/rectal swabs (99
257 individuals, $n=655$), blood/plasma (42 individuals, $n=258$), urine (31 individuals, $n=112$), ocular (16 individuals, $n=50$),
258 breastmilk (4 individuals, $n=90$). Metrics of the full data set are given in Supplementary Table S1.

259
260 Full details of the extracted patient-level covariates are given in Table 2. Recording of fever, days on ICU and days
261 ventilated was largely unavailable. Therefore, no further analysis was performed on these variables. However, it was
262 possible to categorise disease status in all drug quality 1 and 2 papers, either through reports in the manuscript or by
263 contacting corresponding authors. Overall, most patients had mild disease 376 (66.8%), whereas 79 (14.0%) patients had
264 moderate and 84 (14.9%) severe disease. In total 24 (4.3%) asymptomatic patients were reported. The distribution of
265 recorded drug therapies, available for drug quality 1 data and respiratory site samples, is summarised in Supplementary
266 Table S2. Sixty-seven of these patients did not receive antivirals.

267
268 The NLME model fits to the overall data, stratified by sampling site, are provided in Supplementary Table S3 and
269 Supplementary Figure S1. Simulations from the models for each sampling site showing the expected viral load trajectory
270 along with the predicted proportion of samples, that would be below the limit of detection are given in Figure 2. For
271 respiratory sites model-derived AUC, peak viral load and half-life is given in Supplementary Figure S2

272
273 Data on a total of 354 patients with respiratory and/or stool/rectal sampling and drug quality 1 or 2 were available. A
274 forest plot of the parameter estimates from the Cox proportional hazards regression model is provided in Figure 3. Viral
275 clearance was fastest from upper respiratory tract samples and slowest from stool. More sensitive assays (with lower
276 detection limits) were associated with longer time to viral clearance and viral clearance was faster in females, younger
277 patients and those who were asymptomatic.

278
279 Regarding antiviral therapies, only remdesivir (adjusted hazard ratio (AHR) = 9.19, $p<0.001$) and interferons (AHR =
280 2.20, $p=0.015$) were independently associated with faster viral clearance. The effect of interferon alpha and beta
281 (Supplementary Figure S3) was similar and hence these were combined. Lopinavir/ritonavir, ribavirin and interferons

282 were most used and also most used in combination. Adding interaction terms for interferon plus lopinavir/ritonavir,
283 interferon plus ribavirin and lopinavir/ritonavir plus ribavirin in the Cox proportional hazard regression analysis showed a
284 trend towards synergy between interferons and ribavirin in the full dataset (AHR = 6.04, $p=0.006$ Figure 3), as well as in
285 the additional analysis taking in quality assessments to account for potential bias: respiratory data limited to drug quality
286 and in data limited to only viral load quality 1 data (Supplementary Figure S4 and Figure S5). Median sampling
287 frequency in the main survival dataset was 1 day but there was a skewed distribution of sampling frequencies with the
288 mean being 1.9 days and 4.8% of sampling frequencies being greater than 3 days. The main analysis was repeated
289 excluding events with sampling frequencies over 3 days to check for potential bias caused by interval censoring, but the
290 main effect sizes were similar (Figure S6).

291

292 Covariate relationships and drug effects were explored through NLME modelling with parameter estimates of the model
293 given in Supplementary Table S4 along with visual predictive checks and NPDEs in Figure 4 and Supplementary Figure
294 S7 and visualization of viral area under the curve, peak viral load and half-life derived from the final model in
295 Supplementary Figure S8. Drug effects were estimated to increase δ . Drug regimens containing interferon ($\Delta\text{OFV} = -25.5$,
296 $p<0.001$), lopinavir/ritonavir ($\Delta\text{OFV} = 9.97$, $p=0.0016$) and ribavirin ($\Delta\text{OFV} = -22.2$, $p<0.001$) each improved model fit
297 and so were taken forward to the final multivariable drug model. The estimated small lopinavir/ritonavir effect on delta,
298 although showing significant model improvement in the likelihood ratio test, did not prove to be robustly detected in the
299 bootstrap analysis, with the interval crossing the value consistent with no drug effect (Table S4). Implementing an
300 additional synergy term, as detected in the Cox proportional hazard model, did not improve the NLME model.

301

302 The final model was then used to simulate expected viral trajectories from upper respiratory sampling sites for interferon,
303 and ribavirin monotherapy as well as interferon plus ribavirin combination started at 1, 3, 7 and 10 days post symptom
304 onset (Figure 5). The sample sizes for hypothetical Phase II trials to detect significant differences in viral load versus no
305 treatment after 7 days of therapy are given in Supplementary Table S5.

306

307 DISCUSSION

308 This systematic review and individual level meta-analysis has identified viral load trajectories from 645 individuals aged
309 from the first month of life to 100 years. Data from all major sampling sites showed, that: following symptom onset in
310 most patients, upper respiratory tract viral load has peaked and is declining, whereas in the lower respiratory tract viral
311 load peaks 2-3 days after symptom onset; virus is detectable in stool for at least 2 weeks in 75% of individuals, and virus
312 is detected in low levels in blood, urine, ocular secretions and breast milk (Figure 2). In addition to simulating the
313 expected trajectory of viral load at each site, we were able to simulate the percentage of samples expected to be below a
314 typical detection limit of 10 copies/mL (Figure 2). From this it can be seen, that from day 10 post symptom onset over a

315 quarter of upper respiratory samples have undetectable viral load. This emphasises the importance of early antiviral
316 therapy, and for Phase II trials using viral load as an endpoint to commence therapy in the first few days of symptom onset
317 in order to reliably differentiate antiviral effects from natural viral decline (Figure 5, Supplementary Table S5).

318

319 Although we followed PRISMA guidelines on individual patient-level meta-analysis methods, registered our review with
320 PROSPERO and prospectively published our analysis protocol prior to finalising our search, by including data from case
321 reports, case series and clinical trials it could be argued that the heterogeneous inclusion criteria of these data may bias the
322 treatment effects we estimated. We therefore repeated the primary analysis on subsets of the data based on sampling site,
323 data quality and sampling frequency (Supplementary Figures S4-6) finding that the main effects were consistent. It should
324 be noted that by far the largest drug quality 1 dataset was the clinical trial from Hung et al⁹ with 127 patients randomised
325 to either lopinavir/ritonavir versus lopinavir/ritonavir plus ribavirin plus interferon β , and our second largest drug quality 1
326 group was those confirmed to have received no antiviral drugs (67 patients). In total our NLME dataset contained data on
327 83 patients receiving interferons, 187 patients receiving lopinavir/ritonavir, and 99 patients receiving ribavirin either alone
328 or in combination (Table S2). Therefore, whilst consistency in results with various subgroup analyses indicate
329 confounding related to heterogeneous data is unlikely to have biased our main findings, the heterogeneity in drug and drug
330 combination studies meant modelling was required to tease out individual drug effects.

331

332 A heterogeneous range of antivirals, administered in different combinations, was observed in our data (Supplementary
333 Table S2) meaning multivariable modelling of time to viral clearance was used to tease out individual drug effects. No
334 antiviral activity was seen for chloroquine/hydroxychloroquine, azithromycin, lopinavir/ritonavir, umifenovir and
335 thymalfasin. However, remdesivir and interferons were both independently associated with shorter time to viral clearance
336 (Figures 3, S4 and S5). Remdesivir did not however significantly decrease δ in the NLME model, but this is likely due to
337 the low number of included patients.

338

339 Our most interesting finding is the promising antiviral activity of interferons, possibly due to low endogenous interferon
340 levels induced by SARS-CoV-2^{23, 24}. Interferons (alpha and beta) have shown extensive *in vitro* activity against Severe
341 acute respiratory syndrome-1 (SARS-CoV-1) and Middle East respiratory syndrome coronavirus (MERS-CoV)²⁵,
342 ²⁶. However, this has not translated into clinical effectiveness in MERS-CoV²⁵, although results from one trial are still
343 pending²⁷. Although recent data suggests interferon beta may be more potent than alpha against SARS-CoV-2 *in vitro*²⁸,
344 possibly due to higher selective indices for interferon-beta 1b, upon finding similar effects of interferon alpha and beta in
345 our primary analysis (Figure S3), we decided to combine the interferon effect to better explore drug combinations. In the
346 Cox proportional hazard analysis, consistent across data qualities and sampling site combinations, we found either a
347 significant or trend towards significant synergistic activity of interferon plus ribavirin (Figures 3, 4, S4). An extensive

348 body of literature exists to show both interferon alpha and beta are synergistic with ribavirin *in vitro* against both SARS-
349 CoV-1 and MERS-CoV²⁵. This synergy, however, was not confirmed when tested in the NLME analysis, indicating that
350 the detected synergistic effect from the time to viral clearance analysis might be confounded. Correlations in the timing for
351 start of drug treatment could be one confounder that is corrected for in the NLME approach. The time-dependant analysis
352 from the NLME model suggests an additive effect for interferon and ribavirin, rather than a synergistic effect. Thus,
353 combining interferons with a nucleoside analogue, possibly remdesivir or favipiravir as less toxic alternatives to ribavirin,
354 is a potentially promising combination for viral load suppression. In our secondary analysis, we included interferon plus
355 ribavirin in the NLME model and simulations show that virus should be suppressed 2-3 days faster compared to no
356 treatment (Figure 5). However, it must be noted that recent evidence from the WHO SOLIDARITY trial shows that
357 interferons were associated with a trend to increased mortality²⁹ whereas an unpublished press release reports inhaled
358 interferon- β to be beneficial³⁰. There is a clear need for a well-designed Phase II trial on interferons in early disease to
359 confirm or refute the signal seen in our data.

360
361 Another main finding of our work was the limited antiviral effect of lopinavir/ritonavir, in addition to its lack of
362 significant synergistic effect with either ribavirin or interferons. The protease inhibitor lopinavir had a modest but
363 consistent *in vitro* activity against the major coronaviruses, including SARS-CoV-2, although activity is confined to
364 concentrations at the upper end of the clinically achievable range¹. Whilst lopinavir significantly improved model fit
365 when increasing δ , the bootstrap lower boundary crossed the threshold of no drug effect (Table S4), and our simulations
366 suggest monotherapy studies would require well over 500 participants per arm just to show antiviral activity. As recent
367 Phase III trials have now conclusively shown, lopinavir/ritonavir is ineffective in monotherapy^{29,31}. It remains to be seen
368 whether lopinavir/ritonavir may be useful in combinations, however. In SARS-CoV-1 lopinavir/ritonavir plus ribavirin
369 was found to be synergistic *in vitro* and when initiated immediately upon diagnosis led to a significant decrease in
370 mortality compared to historical controls^{32,33}. Early post-exposure prophylaxis against Middle East Respiratory Syndrome
371 (MERS-CoV) in healthcare workers showed that lopinavir/ritonavir plus ribavirin reduced the incidence of infection from
372 28% to 0%³⁴. The lopinavir/ritonavir plus ribavirin combination has therefore been the basis for many clinical trials and
373 treatment protocols, but our findings suggest that it may not be as useful in SARS-CoV-2 (Figure 3).

374
375 The antiviral effects of remdesivir *in vitro* are well established and despite only being able to extract individual patient-
376 level data on six patients, it produced a significantly faster viral clearance in the primary analysis (Figure 3). Despite in
377 some cases showing promising *in vitro* activity, we did not find significant antiviral effects of azithromycin,
378 chloroquine/hydroxychloroquine, thymalfasin or umifenovir. In the case of hydroxychloroquine and azithromycin the raw
379 viral load data from the heavily criticised study by Gautret et al³⁵ was included, but contrary to the original analysis we
380 found no clinical antiviral activity of either drug and, in the case of hydroxychloroquine, a trend towards slower viral
381 clearance. The reason for this difference in interpretation appears to stem from using time since symptom onset as opposed

382 to time since starting drug and with untreated patients being monitored from an earlier day-post symptom onset. This
383 example highlights the necessity of accounting for the time course of the infection when analysing viral loads.

384

385 In our secondary NLME analysis the simplified target cell limited model provided a good fit to data from each sampling
386 site. In many cases this approximated a mono-exponential decay, but in others, particularly in lower respiratory tract, there
387 was a pronounced peak in the first days following symptom onset. The model was stable with high inter-individual
388 variability on V_0 and β , reflecting the fact that relative changes in these parameters lead to the initial part of the curve
389 either rising then falling (in situations when $V_0 \approx -\beta$) or approximately monoexponentially declining (when $V(0) \gg -\beta$). In
390 addition, we found the model to be less sensitive to changes in γ , meaning it can take a wide range of values with little
391 influence on model fit, hence we did not estimate an inter-individual variability term on it. Increasing age was associated
392 with significantly slower δ , and there was a small effect of male sex also being associated with slower δ (Table S4). The
393 age effect translates to a 5-year-old having a viral decay terminal half-life of 1.0 day, a 47-year-old (median age in our
394 population) 1.18 days and a 90-year-old 1.24 days. Hence a child has an almost 15% faster viral clearance than a middle-
395 aged adult, and almost 20% faster than an elderly person.

396

397 In contrast to authors who have estimated parameters for more mechanistic models³⁶, we estimated all drug effects to
398 increase δ , which implies a mode of action relating to inhibition of viral replication or stimulation of viral clearance
399 mechanisms. Whilst for most of the drugs studied this may be reasonable, entry inhibitors may be more appropriately
400 described by inhibition of γ , which may not be statistically identifiable with the data possible to collect in the clinical
401 setting. Despite this potential limitation, we found similar agents (combinations including interferons and ribavirin) to
402 those identified in the primary analysis of time-to viral clearance.

403

404 The major limitation of our work is the lack of clinical trial data and lack of data on potentially important re-purposing
405 agents such as favipiravir and nitazoxanide and that only one of the authors of a major clinical trial agreed to share their
406 data⁹. Through applying quality assessment criteria on drug history and assay reporting, pre-specifying our analysis in our
407 protocol and PROSPERO registration before undertaking Cox proportional hazards and NLME modelling we aimed to
408 reduce possible bias in the heterogenous data available. Whilst we were able to extract a limited common demographics
409 set, particularly in the high-quality data subset (age, sex, disease severity, antiviral drug histories), our data may be limited
410 by other non-antiviral medications that were not fully reported in the included papers. Furthermore, as many of our
411 included papers were on patients with mild or no symptoms and only contained data on one patient reported to have died,
412 we were unable to study associations of viral load and mortality. Viral load measured by PCR is not necessarily infectious
413 virus, and recently it has been shown that only in samples above 10^7 copies/mL can SARS-CoV-2 be cultured²⁹.

414 Therefore, our data should preferably be used to study viral trajectories in relation to antiviral therapy rather than to infer
415 probability of transmission.

416

417 The detection of viable virus might be overcome through whole genome sequencing and the detection of subgenomic
418 RNA. This has however only been conducted in a single study, included in our review. Woelfel et al.³⁷ showed through E
419 gene subgenomic RNA quantification and relating it to the entire virus genome RNA, that presence of subgenomic RNA
420 fragments can be a hint for active viral replication and thus active infection. More recent studies by Alexandersen et al³⁸
421 and van Kampen et al³⁹ however detected subgenomic RNA up to 22 days after onset of symptoms. It is postulated this
422 was related to subgenomic RNA being rather stable and associated with cellular membranes and thus detection of
423 subgenomic RNAs in clinical samples does not necessarily indicate viral activity. Future controlled studies of subgenomic
424 RNA levels in patients on and off antiviral therapies are urgently required to better understand this potential biomarker of
425 drug effect.

426

427 In conclusion, this individual patient level meta-analysis has yielded useful insights into SARS-CoV-2 viral dynamics. A
428 model-based description of viral trajectories in different sampling sites has been elucidated, and we have found covariates
429 such as increasing age, disease severity and male sex to be associated with slower viral clearance. Our review firmly
430 establishes a role for early viral suppression in the management of SARS-CoV-2 and an important signal as to the possible
431 benefits of interferons as a component of antiviral therapy has been found. It has been shown that viral dynamic models
432 such as ours can increase the power to detect drug effects due to their utilisation of serial measures⁴⁰ and our model should
433 be useful to others in both the design and analysis of future Phase II trials, hence the model code and raw data from this
434 analysis is made available.

435

436 DATA AVAILABILITY

437 The final dataset is available at: <https://github.com/ucl-pharmacometrics/SARS-CoV-2-viral-dynamic-meta-analysis>

438

439 CODE AVAILABILITY

440 Model code is available at: <https://github.com/ucl-pharmacometrics/SARS-CoV-2-viral-dynamic-meta-analysis>

441

442

443 FIGURE LEGENDS

444 Figure 1: PRISMA diagram detailing the systematic search results.

445

446 Figure 2: Model-predicted viral load trajectories at each sample site studied.

447 Black lines are the median predictions, with shaded areas representing the 95% prediction interval. The percentage of
448 samples that are predicted to be below a typical limit of detection (10 copies/mL) are given in 2-daily time bins on each
449 plot.

450

451 Figure 3: Multivariable Cox proportional hazard results on all drug quality 1 and drug quality 2 data from respiratory and
452 stool/rectal sampling sites. Adjusted hazard ratios exceeding 1 indicate virus being more likely to become undetectable.

453

454 Figure 4: Visual predictive checks for the NLME model fitted to viral load data to each sampling

455 site. For each site a plot of model simulations compared with observations is given for both the continuous data (upper)
456 and the fraction of samples below the limit of detection (lower). Black circles are observed viral loads, purple shaded area
457 is the 95% prediction interval of the simulated 2.5th and 97.5th percentile for comparison with the observed 2.5 and 97.5th
458 percentile (dashed lines). The blue shaded area is the 95% prediction interval of the 50th percentile to compare with the
459 continuous black line. In the lower plot the observed proportion of samples below the lower limit of detection (LLOD) are
460 shown as a black line and compared with the 95% prediction interval of the model predicted proportion of samples below
461 the LLOD (green shaded area).

462

463 Figure 5: Simulated viral load trajectories.

464 Simulations with a dummy population equally distributed between 50 and 100 years, and equal male/female ratio were
465 performed for each scenario. Drugs were started at day 1 (blue), day 3 (orange), day 7 (green) or day 10 (red) post
466 symptom onset. Mean black line and error bars represent simulations of the dummy population without drug treatment.
467 Coloured mean lines and error bars represent the respective drug regimen. Percentage values represent expected
468 proportion of samples below the limit of detection for no drug (black) versus drug therapy (coloured) at each time point.

REFERENCES

1. Arshad U, *et al.* Prioritization of Anti-SARS-Cov-2 Drug Repurposing Opportunities Based on Plasma and Target Site Concentrations Derived from their Established Human Pharmacokinetics. *Clin Pharmacol Ther.* (2020)
2. To KK, *et al.* Temporal profiles of viral load in posterior oropharyngeal saliva samples and serum antibody responses during infection by SARS-CoV-2: an observational cohort study. *Lancet Infect Dis* **20** 565-574. (2020)
3. He X, *et al.* Temporal dynamics in viral shedding and transmissibility of COVID-19. *Nat Med* **26** 672-675. (2020)
4. Rajpal A, Rahimi L, Ismail-Beigi F. Factors Leading to High Morbidity and Mortality of COVID-19 in Patients with Type 2 Diabetes. *J Diabetes.* (2020)
5. Fishman JA, Grossi PA. Novel Coronavirus-19 (COVID-19) in the immunocompromised transplant recipient: #Flatteningthecurve. *Am J Transplant* **20** 1765-1767. (2020)
6. Zheng S, *et al.* Viral load dynamics and disease severity in patients infected with SARS-CoV-2 in Zhejiang province, China, January-March 2020: retrospective cohort study. *BMJ* **369** m1443. (2020)
7. Kamal MA, *et al.* A drug-disease model describing the effect of oseltamivir neuraminidase inhibition on influenza virus progression. *Antimicrob Agents Chemother* **59** 5388-5395. (2015)
8. Kim JY, *et al.* Viral Load Kinetics of SARS-CoV-2 Infection in First Two Patients in Korea. *J Korean Med Sci* **35** e86. (2020)

9. Hung IF, *et al.* Triple combination of interferon beta-1b, lopinavir-ritonavir, and ribavirin in the treatment of patients admitted to hospital with COVID-19: an open-label, randomised, phase 2 trial. *Lancet* **395** 1695-1704. (2020)
10. Recovery trial. Statement from the Chief Investigators of the Randomised Evaluation of COVID-19 thERapY (RECOVERY) Trial on lopinavir-ritonavir. 2020 [cited 29.06.2020] Available from: https://www.recoverytrial.net/files/lopinavir-ritonavir-recovery-statement-29062020_final.pdf
11. Stewart LA, *et al.* Preferred Reporting Items for Systematic Review and Meta-Analyses of individual participant data: the PRISMA-IPD Statement. *JAMA* **313** 1657-1665. (2015)
12. Rohatgi A. Webplotdigitizer: Version 4.2. 2019 [cited] Available from: <https://automeris.io/WebPlotDigitizer>.
13. Vogels CBF, *et al.* Analytical sensitivity and efficiency comparisons of SARS-COV-2 qRT-PCR primer-probe sets. *medRxiv* 2020.2003.2030.20048108. (2020)
14. Chu DKW, *et al.* Molecular Diagnosis of a Novel Coronavirus (2019-nCoV) Causing an Outbreak of Pneumonia. *Clin Chem* **66** 549-555. (2020)
15. Grambsch PM, Therneau TM. Proportional hazards tests and diagnostics based on weighted residuals. *Biometrika* **81** 515-526. (1994)
16. R Core Team. A language and environment for statistical computing (version 3.6.3). R Foundation for Statistical Computing, Vienna, Austria. 2019 [cited] Available from:

- Accepted Article
17. Baccam P, Beauchemin C, Macken CA, Hayden FG, Perelson AS. Kinetics of influenza A virus infection in humans. *J Virol* **80** 7590-7599. (2006)
 18. Anguelova M, Karlsson J, Jirstrand M. Minimal output sets for identifiability. *Math Biosci* **239** 139-153. (2012)
 19. Kim KS, *et al.* Modelling SARS-CoV-2 Dynamics: Implications for Therapy. *medRxiv* 2020.2003.2023.20040493. (2020)
 20. Beal SLS, L.B.; Boeckmann,A.J.; Bauer, R.J. NONMEM 7.4 users guides. (1989 -2018) [cited]Available from: 10.1128/AAC.00069-15
 21. Nguyen TH, *et al.* Model Evaluation of Continuous Data Pharmacometric Models: Metrics and Graphics. *CPT Pharmacometrics Syst Pharmacol* **6** 87-109. (2017)
 22. Beal SL. Ways to Fit a PK Model with Some Data Below the Quantification Limit. *Journal of Pharmacokinetics and Pharmacodynamics* **28** 481-504. (2001)
 23. Blanco-Melo D, *et al.* Imbalanced Host Response to SARS-CoV-2 Drives Development of COVID-19. *Cell* **181** 1036-1045 e1039. (2020)
 24. Chu H, *et al.* Comparative replication and immune activation profiles of SARS-CoV-2 and SARS-CoV in human lungs: an ex vivo study with implications for the pathogenesis of COVID-19. *Clin Infect Dis.* (2020)

25. Zeitlinger M, *et al.* Pharmacokinetics/Pharmacodynamics of Antiviral Agents Used to Treat SARS-CoV-2 and Their Potential Interaction with Drugs and Other Supportive Measures: A Comprehensive Review by the PK/PD of Anti-Infectives Study Group of the European Society of Antimicrobial Agents. *Clin Pharmacokinet.* (2020)
26. Sheahan TP, *et al.* Comparative therapeutic efficacy of remdesivir and combination lopinavir, ritonavir, and interferon beta against MERS-CoV. *Nat Commun* **11** 222. (2020)
27. Arabi YM, *et al.* Treatment of Middle East Respiratory Syndrome with a combination of lopinavir-ritonavir and interferon-beta1b (MIRACLE trial): study protocol for a randomized controlled trial. *Trials* **19** 81. (2018)
28. Yuan S, *et al.* Broad-Spectrum Host-Based Antivirals Targeting the Interferon and Lipogenesis Pathways as Potential Treatment Options for the Pandemic Coronavirus Disease 2019 (COVID-19). *Viruses* **12**. (2020)
29. Pan H, *et al.* Repurposed antiviral drugs for COVID-19 –interim WHO SOLIDARITY trial results. *medRxiv* 2020.2010.2015.20209817. (2020)
30. Synairgen plc. Interim results for the six months ended 30 June 2020. 2020 [cited]Available from: <https://www.synairgen.com/wp-content/uploads/2020/09/200929-Synairgen-Interim-Results-final.pdf>
31. Recovery Collaborative Group. Lopinavir-ritonavir in patients admitted to hospital with COVID-19 (RECOVERY): a randomised, controlled, open-label, platform trial. *Lancet.* (2020)

32. Chu CM, *et al.* Role of lopinavir/ritonavir in the treatment of SARS: initial virological and clinical findings. *Thorax* **59** 252-256. (2004)
33. Chan KS, *et al.* Treatment of severe acute respiratory syndrome with lopinavir/ritonavir: a multicentre retrospective matched cohort study. *Hong Kong Med J* **9** 399-406. (2003)
34. Park SY, *et al.* Post-exposure prophylaxis for Middle East respiratory syndrome in healthcare workers. *J Hosp Infect* **101** 42-46. (2019)
35. Gautret P, *et al.* Hydroxychloroquine and azithromycin as a treatment of COVID-19: results of an open-label non-randomized clinical trial. *Int J Antimicrob Agents* **56** 105949. (2020)
36. Goncalves A, *et al.* Timing of antiviral treatment initiation is critical to reduce SARS-CoV-2 viral load. *CPT Pharmacometrics Syst Pharmacol.* (2020)
37. Wolfel R, *et al.* Virological assessment of hospitalized patients with COVID-2019. *Nature* **581** 465-469. (2020)
38. Alexandersen S, Chamings A, Bhatta TR. SARS-CoV-2 genomic and subgenomic RNAs in diagnostic samples are not an indicator of active replication. *medRxiv* 2020.2006.2001.20119750. (2020)
39. van Kampen JJA, *et al.* Shedding of infectious virus in hospitalized patients with coronavirus disease-2019 (COVID-19): duration and key determinants. *medRxiv* 2020.2006.2008.20125310. (2020)

- Accepted Article
40. Laouenan C, Guedj J, Mentre F. Clinical trial simulation to evaluate power to compare the antiviral effectiveness of two hepatitis C protease inhibitors using nonlinear mixed effect models: a viral kinetic approach. *BMC Med Res Methodol* **13** 60. (2013)
 41. Kam KQ, *et al.* A Well Infant With Coronavirus Disease 2019 With High Viral Load. *Clin Infect Dis* **71** 847-849. (2020)
 42. Liu Y, *et al.* Clinical and biochemical indexes from 2019-nCoV infected patients linked to viral loads and lung injury. *Sci China Life Sci* **63** 364-374. (2020)
 43. Lim J, *et al.* Case of the Index Patient Who Caused Tertiary Transmission of COVID-19 Infection in Korea: the Application of Lopinavir/Ritonavir for the Treatment of COVID-19 Infected Pneumonia Monitored by Quantitative RT-PCR. *J Korean Med Sci* **35** e79. (2020)
 44. Pan Y, Zhang D, Yang P, Poon LLM, Wang Q. Viral load of SARS-CoV-2 in clinical samples. *Lancet Infect Dis* **20** 411-412. (2020)
 45. Zhang W, *et al.* Molecular and serological investigation of 2019-nCoV infected patients: implication of multiple shedding routes. *Emerg Microbes Infect* **9** 386-389. (2020)
 46. Xu T, *et al.* Clinical features and dynamics of viral load in imported and non-imported patients with COVID-19. *Int J Infect Dis* **94** 68-71. (2020)
 47. Chen W, *et al.* Detectable 2019-nCoV viral RNA in blood is a strong indicator for the further clinical severity. *Emerg Microbes Infect* **9** 469-473. (2020)

48. Young BE, *et al.* Epidemiologic Features and Clinical Course of Patients Infected With SARS-CoV-2 in Singapore. *JAMA.* (2020)
49. Shen C, *et al.* Treatment of 5 Critically Ill Patients With COVID-19 With Convalescent Plasma. *JAMA.* (2020)
50. Wan R, Mao ZQ, He LY, Hu YC, Wei C. Evidence from two cases of asymptomatic infection with SARS-CoV-2: Are 14 days of isolation sufficient? *Int J Infect Dis* **95** 174-175. (2020)
51. Lescure FX, *et al.* Clinical and virological data of the first cases of COVID-19 in Europe: a case series. *Lancet Infect Dis* **20** 697-706. (2020)
52. Xu Y, *et al.* Characteristics of pediatric SARS-CoV-2 infection and potential evidence for persistent fecal viral shedding. *Nat Med* **26** 502-505. (2020)
53. Han MS, *et al.* Sequential analysis of viral load in a neonate and her mother infected with SARS-CoV-2. *Clin Infect Dis.* (2020)
54. Wyllie AL, *et al.* Saliva is more sensitive for SARS-CoV-2 detection in COVID-19 patients than nasopharyngeal swabs. *medRxiv* 2020.2004.2016.20067835. (2020)
55. Cheng CY, *et al.* Lopinavir/ritonavir did not shorten the duration of SARS CoV-2 shedding in patients with mild pneumonia in Taiwan. *J Microbiol Immunol Infect* **53** 488-492. (2020)

56. Yang Y, *et al.* Evaluating the accuracy of different respiratory specimens in the laboratory diagnosis and monitoring the viral shedding of 2019-nCoV infections. *medRxiv* 2020.2002.2011.20021493. (2020)
57. Yang JR, *et al.* Persistent viral RNA positivity during the recovery period of a patient with SARS-CoV-2 infection. *J Med Virol.* (2020)
58. Covid- Investigation Team. Clinical and virologic characteristics of the first 12 patients with coronavirus disease 2019 (COVID-19) in the United States. *Nat Med* **26** 861-868. (2020)
59. Lui G, *et al.* Viral dynamics of SARS-CoV-2 across a spectrum of disease severity in COVID-19. *J Infect* **81** 318-356. (2020)
60. Hu Y, *et al.* A report of three COVID-19 cases with prolonged viral RNA detection in anal swabs. *Clin Microbiol Infect* **26** 786-787. (2020)
61. Seah IYJ, *et al.* Assessing Viral Shedding and Infectivity of Tears in Coronavirus Disease 2019 (COVID-19) Patients. *Ophthalmology* **127** 977-979. (2020)
62. Liu WD, *et al.* Prolonged virus shedding even after seroconversion in a patient with COVID-19. *J Infect* **81** 318-356. (2020)
63. Xing YH, *et al.* Prolonged viral shedding in feces of pediatric patients with coronavirus disease 2019. *J Microbiol Immunol Infect* **53** 473-480. (2020)

64. Qian GQ, *et al.* Duration of SARS-CoV-2 viral shedding during COVID-19 infection. *Infect Dis (Lond)* **52** 511-512. (2020)
65. Kim ES, *et al.* Clinical Course and Outcomes of Patients with Severe Acute Respiratory Syndrome Coronavirus 2 Infection: a Preliminary Report of the First 28 Patients from the Korean Cohort Study on COVID-19. *J Korean Med Sci* **35** e142. (2020)
66. Colavita F, *et al.* SARS-CoV-2 Isolation From Ocular Secretions of a Patient With COVID-19 in Italy With Prolonged Viral RNA Detection. *Ann Intern Med* **173** 242-243. (2020)
67. Hill KJ, *et al.* The index case of SARS-CoV-2 in Scotland. *J Infect* **81** 147-178. (2020)
68. Huang Y, *et al.* SARS-CoV-2 Viral Load in Clinical Samples from Critically Ill Patients. *Am J Respir Crit Care Med* **201** 1435-1438. (2020)
69. Zhou R, *et al.* Viral dynamics in asymptomatic patients with COVID-19. *Int J Infect Dis* **96** 288-290. (2020)
70. Qi L, *et al.* Factors associated with the duration of viral shedding in adults with COVID-19 outside of Wuhan, China: a retrospective cohort study. *Int J Infect Dis* **96** 531-537. (2020)
71. Yuan C, *et al.* Viral loads in throat and anal swabs in children infected with SARS-CoV-2. *Emerg Microbes Infect* **9** 1233-1237. (2020)

72. Huang JT, *et al.* Chronological Changes of Viral Shedding in Adult Inpatients with COVID-19 in Wuhan, China. *Clin Infect Dis.* (2020)
73. Kong Y, *et al.* Successful treatment of a centenarian with coronavirus disease 2019 (COVID-19) using convalescent plasma. *Transfus Apher Sci* 102820. (2020)
74. Tam PCK, *et al.* Detectable severe acute respiratory syndrome coronavirus 2 (SARS-CoV-2) in human breast milk of a mildly symptomatic patient with coronavirus disease 2019 (COVID-19). *Clin Infect Dis.* (2020)
75. Yoon JG, *et al.* Clinical Significance of a High SARS-CoV-2 Viral Load in the Saliva. *J Korean Med Sci* **35** e195. (2020)
76. Phan LT, *et al.* Clinical features, isolation, and complete genome sequence of severe acute respiratory syndrome coronavirus 2 from the first two patients in Vietnam. *J Med Virol.* (2020)
77. Klement-Frutos E, *et al.* Early administration of ritonavir-boosted lopinavir could prevent severe COVID-19. *J Infect.* (2020)
78. Gross R, *et al.* Detection of SARS-CoV-2 in human breastmilk. *Lancet* **395** 1757-1758. (2020)

SUPPLEMENTAL FILES

1. Supplemental Material

Table 1 Individual papers included in the Meta-Analysis

Study ID	Country	Sample Type	Assay Gene	No. of Patients	Sampled Patients	Samples per patient median [min -max]	Treatment	Symptom details	Age, years median (IQR) {R}	Sex M (F)	Ref.
1	SGP	URT, Vn, Un, Re, Br	N, Orflab	2	2	14,28	None	Yes	0.5	1 (1)	⁴¹
2	KOR	URT, LRT, Vn, Un, Re	RdRp, E	2	2	98,136	lpvr, other	Yes	55/35	1 (1)	⁸
3	HKG	URT, LRT, Vn	RdRp	23	23	3 [1-24]	lpvr, riba, Ifn	Yes* (not longitudinal)	62 {37-75}*	13 (10)*	²
4	CHN	URT, LRT	N, Orflab	12	5	2	riba, ifn, other	Yes (not longitudinal)	63 (47-65) [10-72]	8 (4)	⁴²
5	KOR	URT	RdRp	1	1	11	lpvr, azit, other	Yes	54	1 (0)	⁴³
6	CHN	URT, LRT	N	80 (2)	2	30,50	-	-	-	-	⁴⁴
7	CHN	URT	N, Orflab	17	17	8 [1-17]	-	Yes (not longitudinal)	59 {26-78}	8 (9)	¹
8	CHN	URT, Re, Vn	S	16	16	1 [1-3]	-	-	-	-	⁴⁵
9	FRA	URT	RdRP, E	36	26	7 [3-7]	cqhcq, azit	-	Mean 45 +/- 22	15 (21)	³⁵

Study ID	Country	Sample Type	Assay Gene	No. of Patients	Sampled Patients	Samples per patient median [min -max]	Treatment	Symptom details	Age, years median (IQR) {R}	Sex M (F)	Ref.
10	CHN	URT	N, Orf1lab	51	50	4 [1-14]	lpvr, Ifn, umif, thym, other	Yes	43 (29-53)	25 (26)	⁴⁶
11	CHN	URT, Vn, Re	N, Orf1lab	6	6	9 [2-19]	-	-	-	5(1)	⁴⁷
12	CHN	URT	N	94	94	3 [1-6]	-	-	46 (33-61)*	47 (47)*	³
13	SGP	URT	N, S, and Orf1lab	18	18	16 [7-25]	lpvr	Yes	47 {31-73}*	9 (9)*	⁴⁸
14	CHN	URT	-	5	5	6	lpvr, Ifn, other	Yes	{36-73}*	3 (2)	⁴⁹
15	CHN	URT	Orf1lab	2	2	7,9	lpvr, riba	Yes	19/36	2 (0)	⁵⁰
16	FRA	URT, Re	RdRp, E, RdRp-IP1, GAPDH	5	5	11 [5-13]	remd	Yes (not longitudinal)	46 (31-48)	3 (2)	⁵¹
17	GER	URT, LRT, Re	RdRP, E	9	9	47 [13-54]	-	Yes	40 (33-49)	8 (1)	³⁷
18	CHN	URT, Re	N, Orf1lab	10	9	11 [2-20]	-	Yes	7 (3-13)	6 (4)	⁵²
19	KOR	URT, Vn, Re,	E	2	2	18,33	None	Yes	0.08, neonate	0 (2)	⁵³

Study ID	Country	Sample Type	Assay Gene	No. of Patients	Sampled Patients	Samples per patient median [min -max]	Treatment	Symptom details	Age, years median (IQR) {R}	Sex M (F)	Ref.
		Un									
20	USA	URT	-	44	19	3 [2-8]	-	-	{23-92}, 61 (mean)*	23 (21)*	⁵⁴
21	TWN	URT, LRT	RdRp1, RdRp2, E, N	5	5	20 [17-24]	lpvr, None	Yes	52 (50-53)	2 (3)	⁵⁵
22	CHN	URT, LRT	-	213	13	7 [4-19]	AVT	Yes	52 (2-86)	108 (105)	⁵⁶
23	CHN	URT	-	1	1	9	inf, cqhcq, other	Yes (not longitudinal)	44	1 (0)	⁵⁷
24	USA	URT	-	12	12	25 [14-49]	remd, other	Yes (not longitudinal)	53 {21-68}	8 (4)	⁵⁸
25	HKG	URT, LRT, Vn, Re	-	11	11	9 [2-22]	lpvr, riba, ifn*	Yes (not longitudinal)	58 (42-70)	7 (4)	⁵⁹
26	CHN	URT, Re	Orf1ab, N	3	3	26 [26-52]	ifn, cqhcq, other	Yes	28 {25-32}	2 (1)	⁶⁰
27	SGP	URT	E	17	17	7 [4-14]	-	Yes*	37 {20-75}*	11 (6)	⁶¹
28	TWN	URT, LRT	N, RdRp, E	1	1	249	-	Yes (not longitudinal)	50	0 (1)	⁶²

Study ID	Country	Sample Type	Assay Gene	No. of Patients	Sampled Patients	Samples per patient median [min -max]	Treatment	Symptom details	Age, years median (IQR) {R}	Sex M (F)	Ref.
29	CHN	URT, Re	-	3	1	35	Ifn and Riba	Yes (not longitudinal)	5 {1.5-6}	2 (1)	⁶³
30	CHN	URT, Re	N, RdRp, E	1	1	63	lpvr, umif, ifn, other	Yes	47	1 (0)	⁶⁴
31	KOR	URT, LRT	E	28	9	13 [8-33]	lpvr, none	Yes*	40 (28-54) {20-73}	15 (13)	⁶⁵
32	ITA	URT	-	1	1	28	-	Yes	65	0 (1)	⁶⁶
33	GBR	URT	-	1	1	13	none	Yes	51	1 (0)	⁶⁷
34	CHN	URT, LRT, Co, Vn, Un, Re	-	16	16	53 [27-106]	-	-	59.5 {26-79}*	13 (3)*	⁶⁸
35	HKG	URT	RdRp	127	127	8 [4-8]	lpvr, riba, ifn	-	51.5 {31.0-62.5}	68 (59)	⁹
36	CHN	URT	N	31	19	2 [1-5]	NA	-	41 {28-60}*	10 (21)	⁶⁹
37	CHN	URT	Orf1ab	147	61	2 [1-6]	AVT	Yes	42.0 (35.0-54.0) {19-81}*	67 (80)	⁷⁰
38	CHN	URT, Re	Orf1ab	54	13	12 [7-20]	NA	Yes	6.8 {2.7-11.7}*	37	⁷¹

Study ID	Country	Sample Type	Assay Gene	No. of Patients	Sampled Patients	Samples per patient median [min -max]	Treatment	Symptom details	Age, years median (IQR) {R}	Sex M (F)	Ref.
										(17)	
39	CHN	URT	Orf1ab	308	10	9 [7-11]	Lpvr, ifn, riba, cqhcq	Yes	63.5 {45-81}*	151 (157)	⁷²
40	CHN	URT	-	1	1	5	other	Yes	100	1 (0)	⁷³
41	AUS	URT, Br	E	2	2	24 [20-28]	none	Yes	0.7/40	1 (1)	⁷⁴
42	KOR	URT, LRT, Un	RdRp	2	2	25	lpvr, cqhcq	Yes	46/65	0 (2)	⁷⁵
43	VNM	URT	RdRp	2	2	2,13	other	Yes	65/27	2 (0)	⁷⁶
44	FRA	URT, LRT, Vn, Re	E	1	1	27	lpvr	-	-	1 (0)	⁷⁷
45	GER	Br	N, Orf1ab	2	2	32,50	NA	Yes	-	0 (2)	⁷⁸

br = breastmilk, Co = conjunctiva, LRT = lower respiratory tract, Re = faecal/rectal/anal, Un = urine, URT = upper respiratory tract, Vn = venous (blood, plasma, serum), - = Not Reported. AVT = anti-viral therapy, cqhcq = chloroquine/ hydroxychloroquine, ifn = interferon, lpvr = lopinavir/ritonavir, remd = remdesivir, riba = ribavarin, umif = umifenivir.

Table 2 Overview extracted variables across different analyses, median [range] (%missing data records). n, number of individuals included.

Descriptive (%missing)	All Data <i>n</i> =645	Cox-PH - Full data set <i>n</i> =354	NLME/ reduced Cox-PH <i>n</i> =317
Age [years]	46 [0.1 – 100] (31.3%)	48 [0.1-100] (0%)	46 [0.1-100] (0%)
Sex [male/female]	217/189 (37%)	215/139 (0%)	182/135 (0%)
ICU admission [yes/no]*	36/371 (36.9%)	8/271 (21.2%)	8/257 (16.4%)
Invasive ventilation [yes/no]*	14/348 (43.9%)	9/262 (23.4%)	5/247 (20.5%)
Death [yes/no]	1/455 (29.3%)	1/330 (6.5%)	1/293 (7.3%)
Disease severity*	(12.7%)	(0%)	(0%)
Asymptomatic	24	19	16
Mild	376	258	239
Moderate	79	52	44
Severe	84	25	18

*There is discord between the reported ICU and mechanical ventilation and disease severity score due to incomplete reporting in some papers. Disease severity was taken from individual reports of disease status in cases where ICU admission and invasive ventilation were not specifically mentioned, and only Disease severity was used in the analyses.

Records identified through
PubMed/EMBASE
search n = 3098

Records identified through
bioRxiv/medRxiv search n = 2874

Records retained after du-
plicates removed n = 2972

Abstract and title screened
for eligibility n = 2972

Records excluded n = 1675

Full-text articles assessed
for eligibility n = 1297

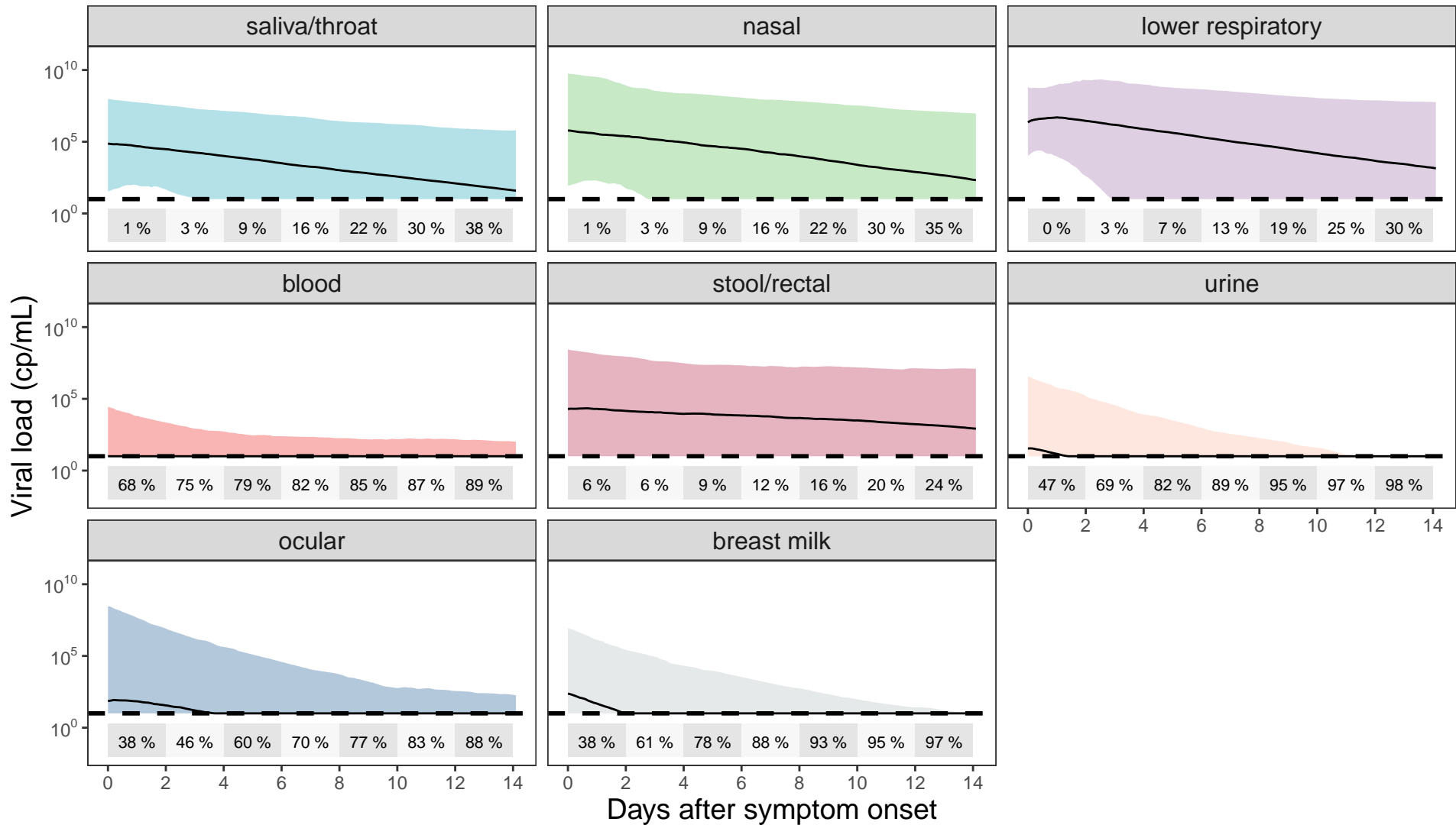
Records excluded
(not containing patient-
level viral load) n = 1252

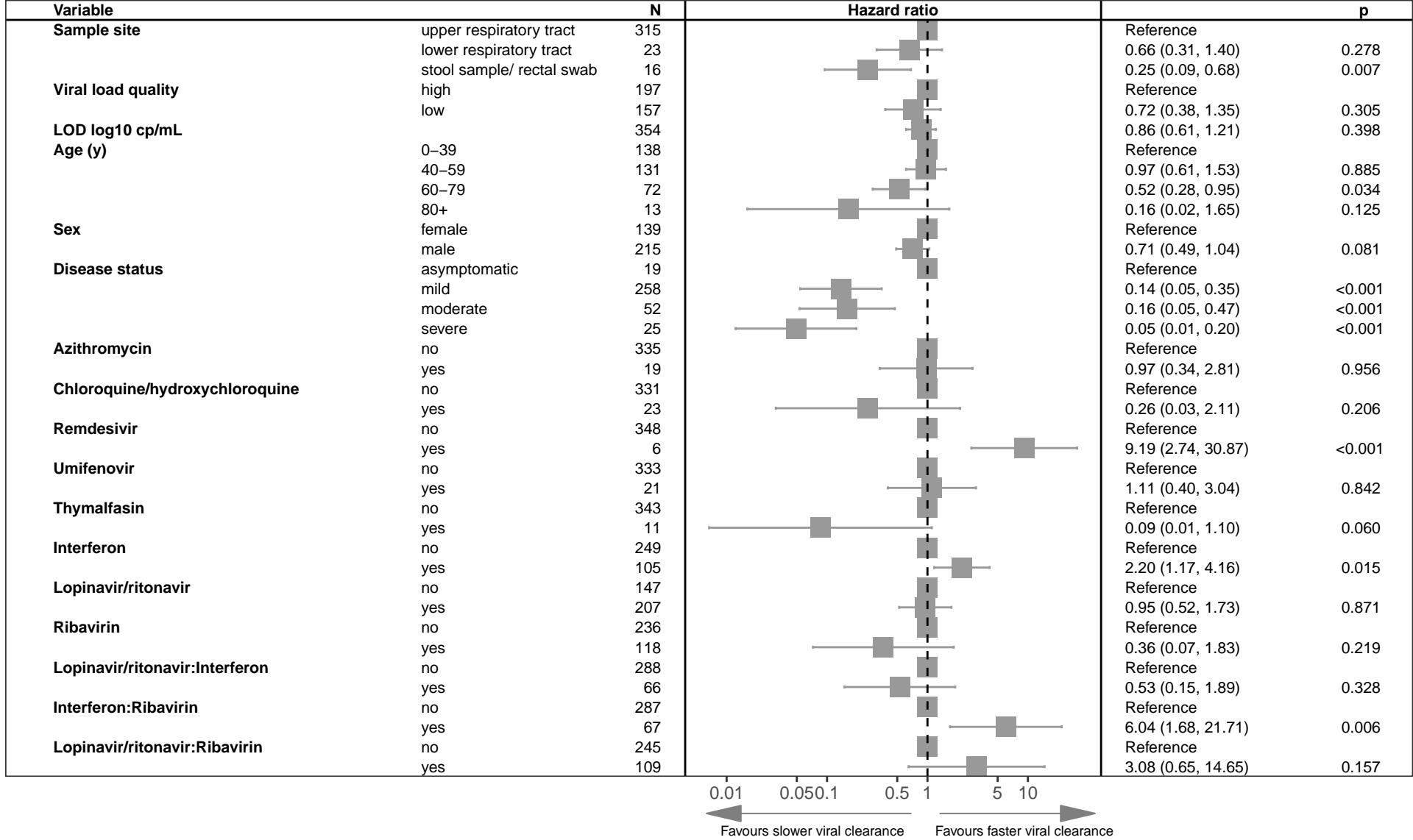
Studies included for
viral load extraction
n = 45 (645 individuals)

Records excluded
(not containing antivi-
ral drug history) n = 13

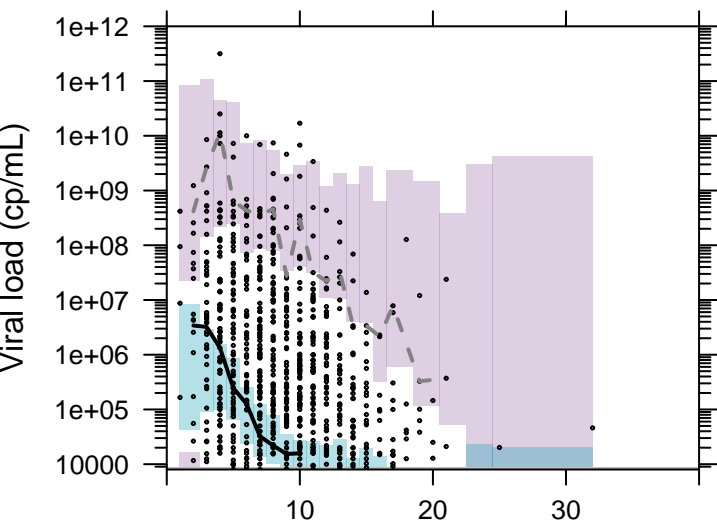
Studies included in quantita-
tive synthesis (meta-analysis)
n = 32 (354 individuals)

Pattern of viral shedding in different sites

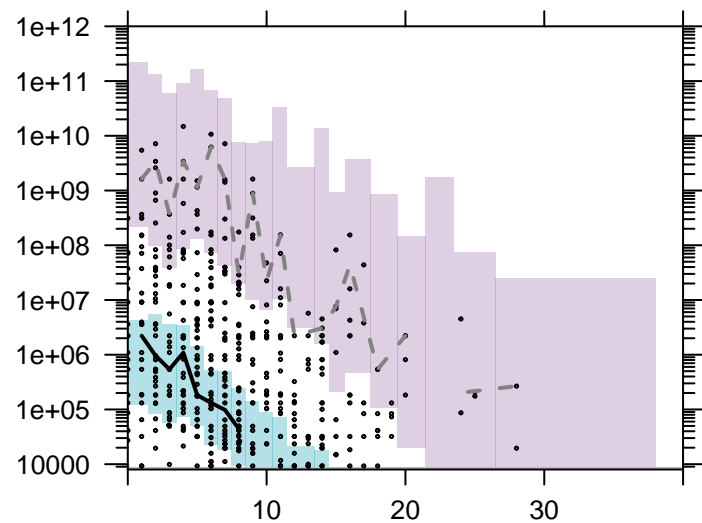




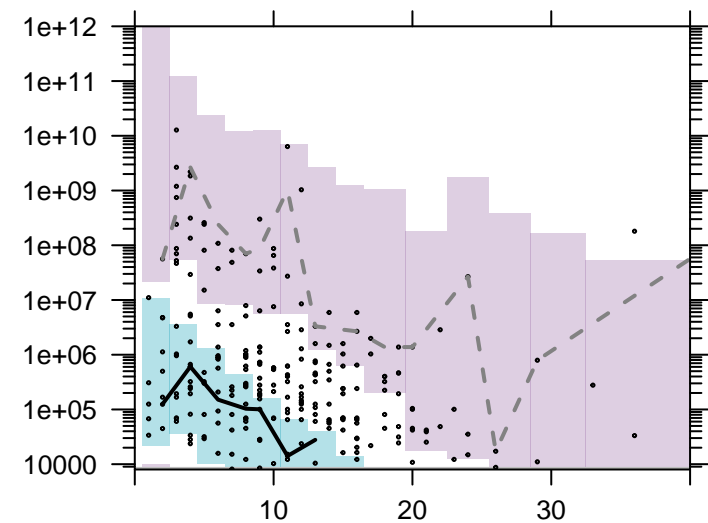
quality 1



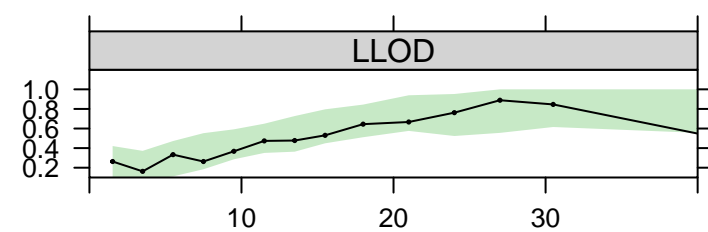
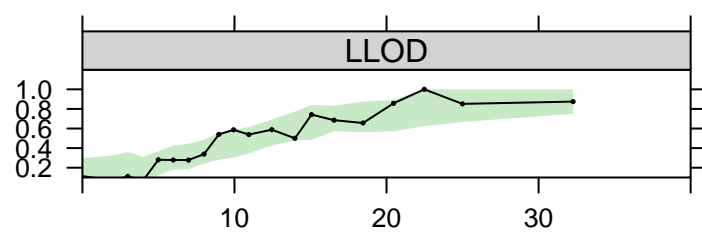
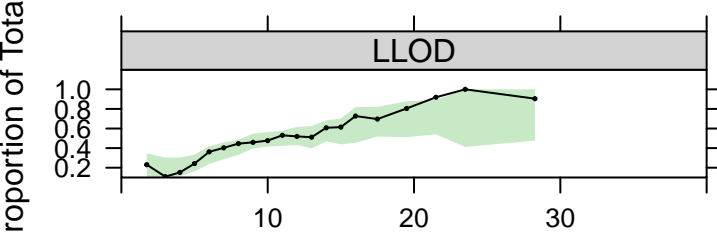
quality 2



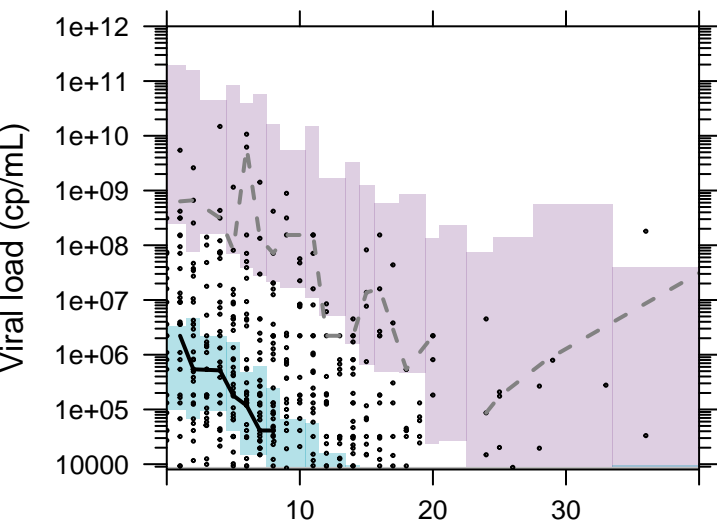
quality 3



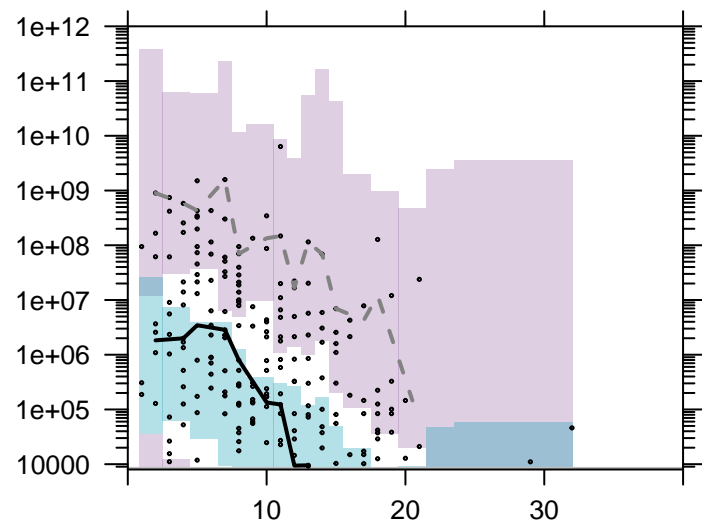
Proportion of Total



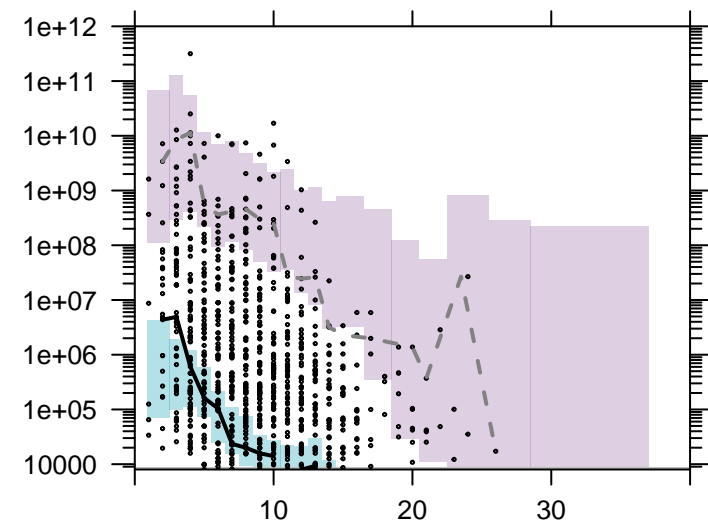
saliva/throat



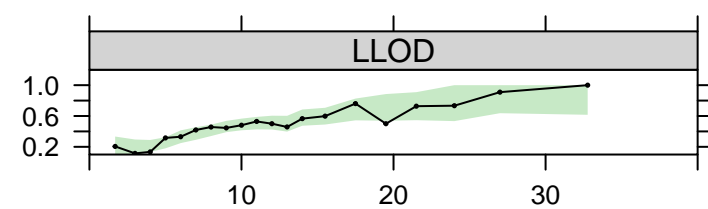
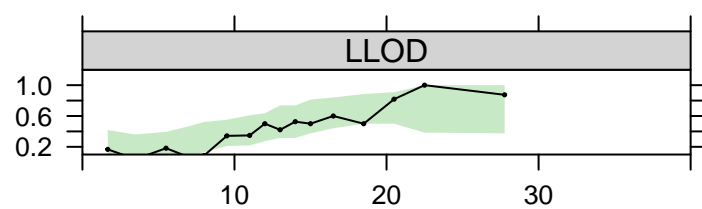
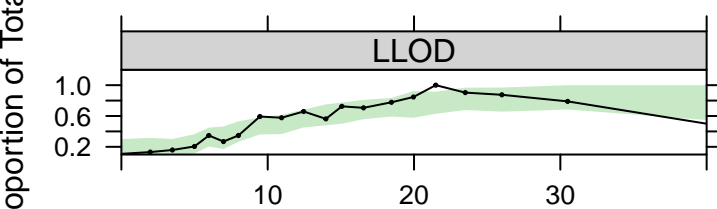
lower respiratory



nasal



Proportion of Total

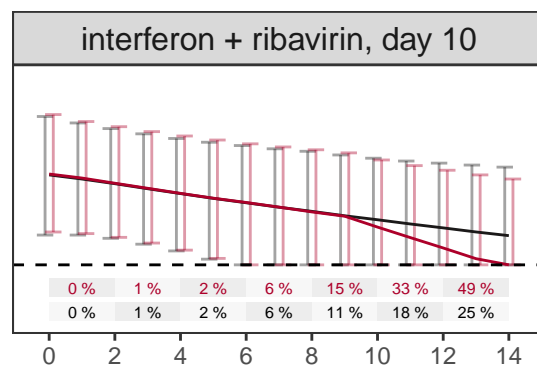
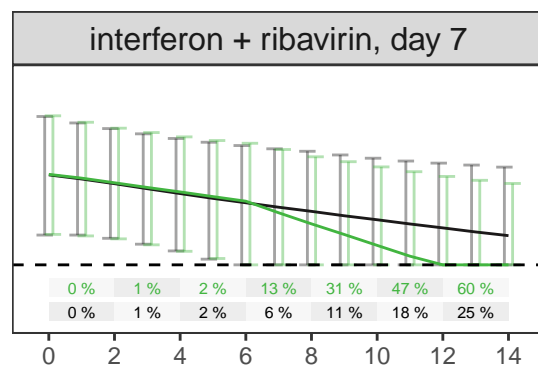
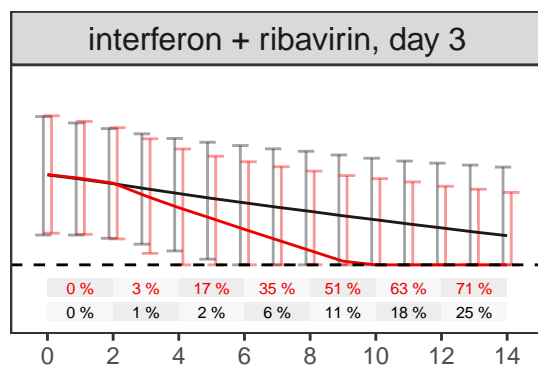
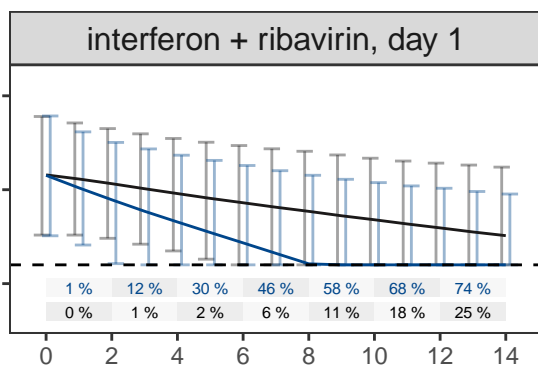
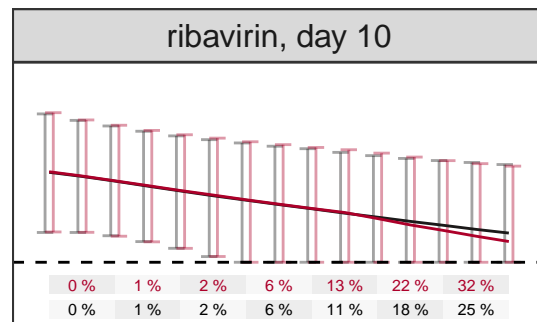
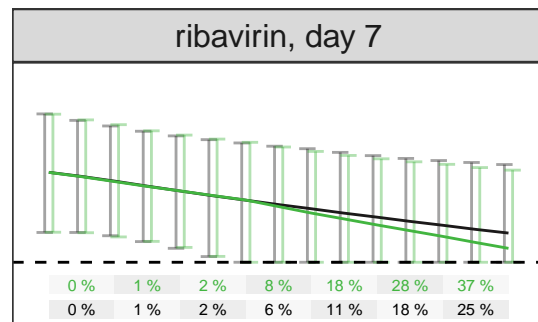
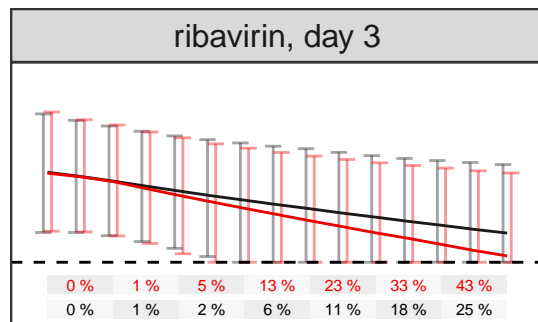
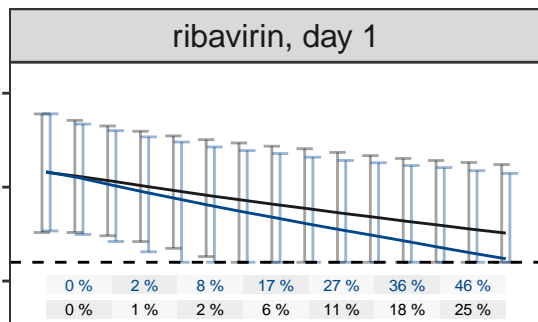
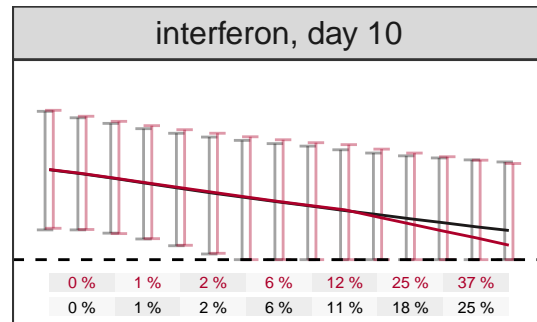
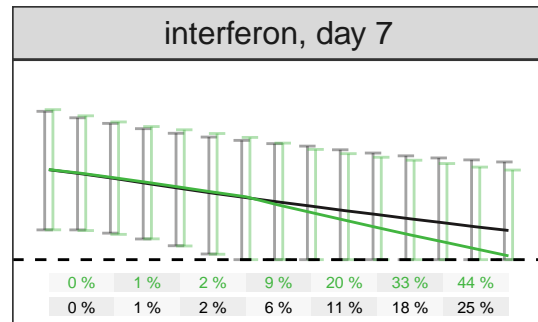
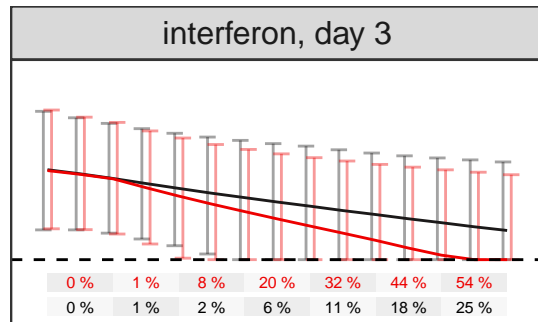
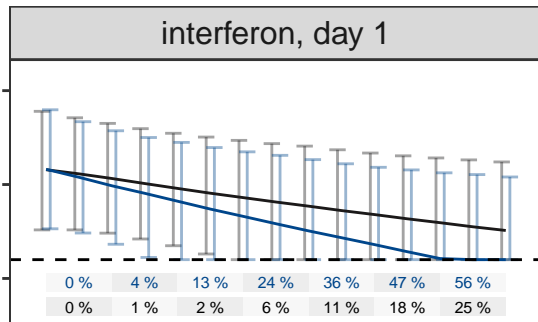


Days after symptom onset

Days after symptom onset

Days after symptom onset

Viral load (cp/mL)



Days after symptom onset